6ICEGE 6th International Conference on Earthquake Geotechnical Engineering
1-4 November 2015
Christchurch, New Zealand

Centrifuge Dynamic Tests on Gravity Retaining Walls: An Insight into Bearing vs Sliding Failure Mechanisms

R. Conti[1], G.S.P. Madabhushi[2], V. Mastronardi[3], G.M.B. Viggiani[4]

ABSTRACT

This paper illustrates an experimental investigation of the seismic behaviour of gravity retaining walls, resting both on rigid and compliant base. The earthquakes applied in the two tests are quite similar - both in magnitude, duration and frequency content - and in both cases they induce permanent displacements of the wall. However, while in the first test (rigid foundation) the wall is constraint to slide over its base, both sliding and rotation of the wall are observed in the second test (compliant foundation), clearly associated to a bearing failure mechanism of the underlying soil. It is found that wall displacements associated to the latter mechanism are substantially larger than those attained by pure sliding. In the light of a Newmark's sliding block procedure, these findings suggest that, depending on the mechanical properties of the supporting soil, the critical acceleration of the wall can be significantly smaller than that associated to a sliding mechanism.

Introduction

Permanent displacements of gravity retaining walls are usually computed through the Newmark (1965) rigid-block analysis (Richards and Elms, 1979). A key ingredient for this method is the yield acceleration, *i.e.* the acceleration corresponding to which the strength of the soil is fully mobilised, which is computed with respect to a given collapse mechanism, assuming a rigid-perfectly plastic behaviour for both the soil and the wall. Knowledge of the yield acceleration is crucial also for the structural design of the wall, as it usually defines the maximum internal forces that the structure may ever experience during an earthquake (Conti *et al*., 2013).

In the light of the Newmark's approach, translational (Ling, 2001) rotational (Zeng & Steedman, 2000) and bearing capacity (Huang, 2005) failure mechanisms have been considered in the literature to compute permanent displacements. However, to the Author's knowledge, no attention has been paid to the relative importance of the three failure mechanisms in computing the yield acceleration of the wall, except for recent experimental studies on cantilevered retaining walls (Kloukinas *et al*., 2013).

The research reported in this note is focused on the physical phenomena that control the dynamic behaviour of gravity retaining walls. The main purpose of this work is to provide further experimental evidence to validate suitable simplified procedures to compute permanent displacements of gravity walls under seismic loading. More in detail, by comparing the results

[1]Research Assistant., Facoltà di Ingegneria, Università Niccolò Cusano, Roma, Italy, riccardo.conti@unicusano.it
[2]Professor, CUED, University of Cambridge, Cambridge, UK, mspg1@eng.cam.ac.uk
[3]Graduate Student, DICII, Università di Roma Tor Vergata, Roma, Italy, valentinamastronardi@libero.it
[4]Professor, DICII, Università di Roma Tor Vergata, Roma, Italy, viggiani@uniroma2.it

from two centrifuge tests on gravity retaining walls, it is shown that, despite the common assumption that sliding is the most critical mechanism, bearing capacity failure of the foundation soil can lead to substantially larger displacements of the wall.

Experimental Work

The experimental program was carried out in the 10 m diameter Turner beam centrifuge of the University of Cambridge. It included two tests (VM01 and VM02) on a model of a gravity retaining wall supporting a backfill of dry loose sand ($D_R \approx 30$ %), both conducted at a centrifugal acceleration of 50g. In test VM01 a rigid aluminum plate of 20 mm thickness was placed between the base of the wall and the underlying layer, in order to force a pure sliding mechanism of the wall in the dynamic stages. In test VM02, on the contrary, a uniform sand layer was realized for both the supporting soil and the backfill (Figure 1).

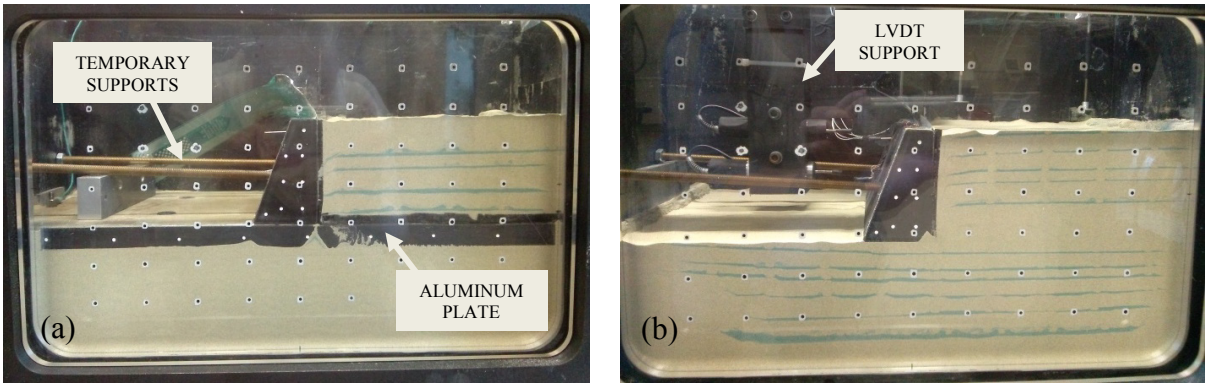

Figure 1. Photograph of the models: (a) test VM01 and (b) test VM02.

Materials

A standard fine silica sand was used to form the models, namely Leighton Buzzard, Fraction E Sand 100/170 (G_S = 2.65, e_{max} = 1.014, e_{min} = 0.613, ϕ_{cv} = 32°). Further details on the mechanical behaviour of the sand under monotonic, cyclic and dynamic loading conditions can be found in Visone and Santucci de Magistris (2009) and Conti and Viggiani (2012).

The wall model was prepared at the Geotechnical Laboratory of University of Roma Tor Vergata using a cement mortar with unit weight of 23 kN/m^3. Figure 2 shows the transversal section of the model, with a trapezoidal shape.

The models were prepared within a rigid container with a Perspex viewing window, allowing soil deformations and wall displacements to be measured during the tests with a Particle Image Velocimetry (PIV) technique. The container has a plan area of 500 mm × 240 mm and a depth of 360 mm. A layer of DUXSEAL of about 40 mm thickness was included between the rigid end walls and the soil in order to prevent generation of P-waves and multiple wave reflection during shaking (absorbing boundary).

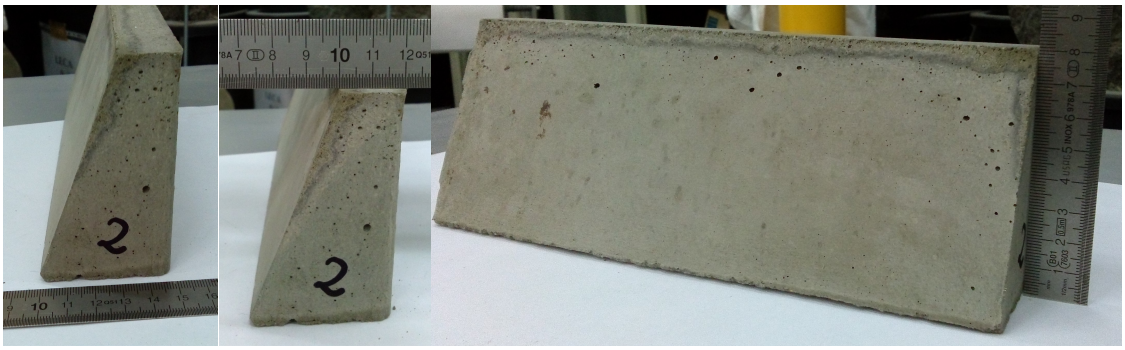

Figure 2. Model of the wall.

Instrumentation

Figure 3 shows the layout of the instrumentation used in the two tests. Accelerations at different locations in the model were measured using miniaturized piezoelectric accelerometers (A); horizontal and vertical accelerations of the wall were recorded using MEMS accelerometers (M), capable of measuring the dynamic acceleration as well as the static acceleration due to gravity and centrifuge swing up. Displacements were measured using LVDTs transducers (LV).

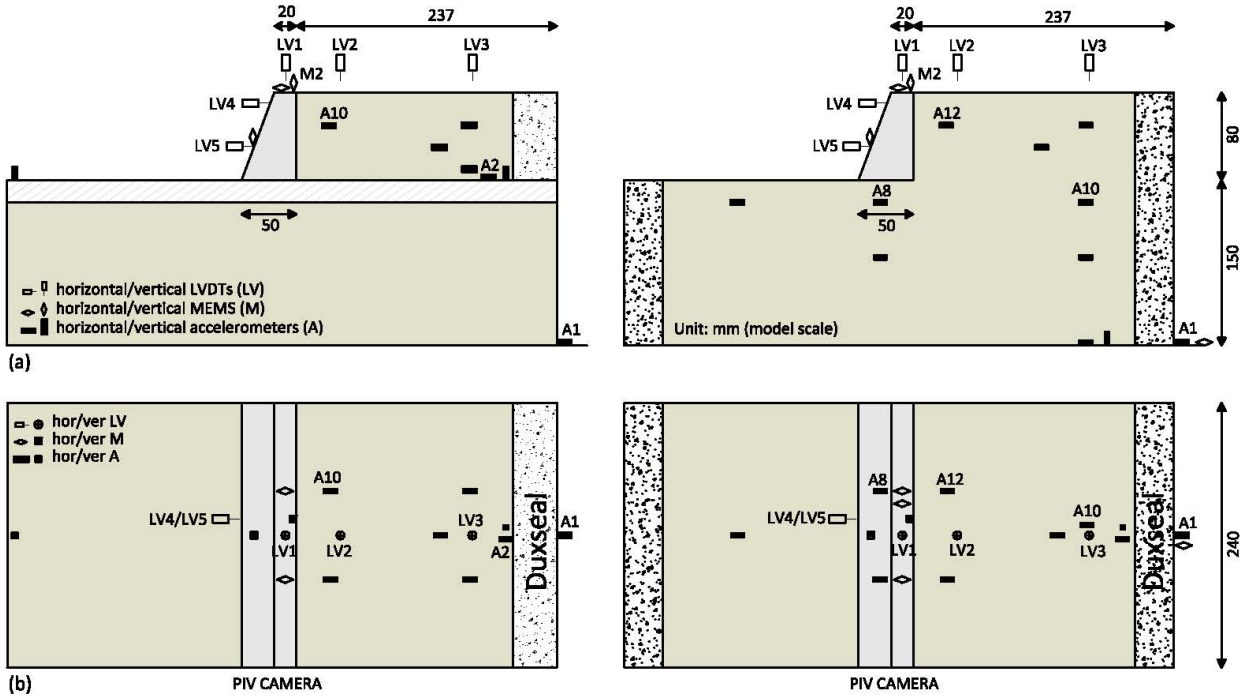

Figure 3. Layout of instrumentation: (a) test VM01 and (b) test VM02.

The horizontal stress distribution at the contact between the wall and the soil was measured using a Tekscan's system, consisting of a flexible sheet of about 0.1 mm thickness with a regular grid of tactile sensors, with spacing of 5.59 mm, allowing pressure distribution to be recorded both during static and dynamic events (Figure 4). Starting from the bottom of the wall and the lateral

side facing the Perspex window, the surface area covered by the Tekscan sheet is 56×89 mm^2 and 56×151 mm^2 in test VM01 and VM02 respectively.

A fast digital camera was used for the PIV analysis, capable of recording 1 Megapixel digital images at 1000 frames per second. More details on application of PIV technique to geotechnical modelling is given by White *et al*. (2003).

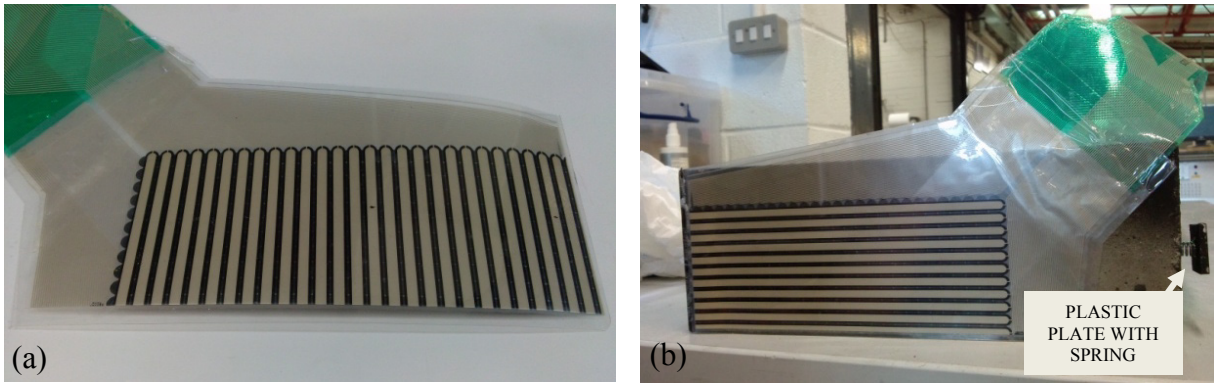

Figure 4. Tekscan's sensors for pressure measurement.

The dynamic input was provided by a Stored Angular Momentum (SAM) actuator. During each test, the model was subjected to a series of trains of approximately sinusoidal waves with different nominal frequencies, f, and amplitudes, a_{max}, and a constant duration (Table 1).

Table 1. Features of the input earthquakes (A1).

Test	Earthquake	model scale			prototype scale		
		f [Hz]	a_{max} [g]	duration [s]	f [Hz]	a_{max} [g]	duration [s]
VM01	EQ1	50	14.82	0.4	1.0	0.30	20
	EQ2	50	15.44	0.4	1.0	0.31	20
	EQ3	60	23.57	0.4	1.2	0.47	20
	EQ4	60	26.12	0.4	1.2	0.52	20
VM02	EQ1	60	25.75	0.4	1.2	0.52	20
	EQ2	60	25.20	0.4	1.2	0.50	20

Model Preparation and Features

An automatic hopper system was used to pluviate the sand into the container. In test VM02 a uniform relative density of about 30 % was achieved within the whole model, while in test VM01 the sand layer below the aluminum plate is much denser ($D_R \approx 80$ %) than the overlying backfill ($D_R \approx 30$ %).

During preparation, temporary rigid supports were used to prevent wall displacements. In order to avoid side effects, the wall is 5 mm shorter than the box width. A plastic black plate with white markers was glued to the lateral side of the wall facing the Perspex window and the PIV camera, while a smaller plate was connected to the opposite side through a spring (Figure 4(b)). Both plates were greased with silicon to minimise friction. Moreover, thin and extensible plastic sheets were used to avoid sand flowing laterally between the wall and the box, but without restraining wall displacements.

LB Sand was glued both to the base of the wall model and to the upper face the aluminium plate. The friction angle at the base of the wall is 29.5° in test VM01, computed from a direct shear test, and equal to the soil friction angle in test VM02. As far as the back side of the wall is concerned, zero friction can be assumed between the soil and the wall due to the presence of the Tekscan sheet for most part of the surface area.

Experimental Observations

A huge amount of experimental data were obtained from both tests, part of them still under elaboration. As far as the static stage is concerned, we will focus solely on the interpretation of the earth pressure measurements, while concentrating on kinematic mechanisms and wall displacements during the dynamic stages. In the following, accelerations are positive rightwards and horizontal displacements of the wall are positive leftwards (see *e.g.,* Figure 1). All results are presented at prototype scale, unless explicitly stated.

Static Stage: Earth Pressure Measurements

Figure 5 shows (a) the time history of contact stresses during the swing up stage at $z = 66$ mm, along four different sections; (b) the horizontal earth pressure distribution in the same sections at the end of the swing up stage; and (c) the contour of horizontal stresses at 50g. Moreover, Figure 5(a) shows the theoretical profiles of the active (σ_a) and at rest (σ_0) horizontal stress, computed from the vertical acceleration measured by M2 assuming $\phi = \phi_{cv}$ as the soil friction angle. During the swing up stage, contact stresses on the wall must increase together with the centrifugal acceleration in the model, being close to σ_a or σ_0 depending on wall displacements. Figures 5(a) and 5(b) show clearly that most of the transducers performed properly during the static stage, the recorded stress being close to the active limit state, except for a few sensors that were not considered in the following elaboration (clean data). The contour map shown in Figure 5(c) was computed by linear interpolation of the available clean data, pointed out by cross markers in the plot.

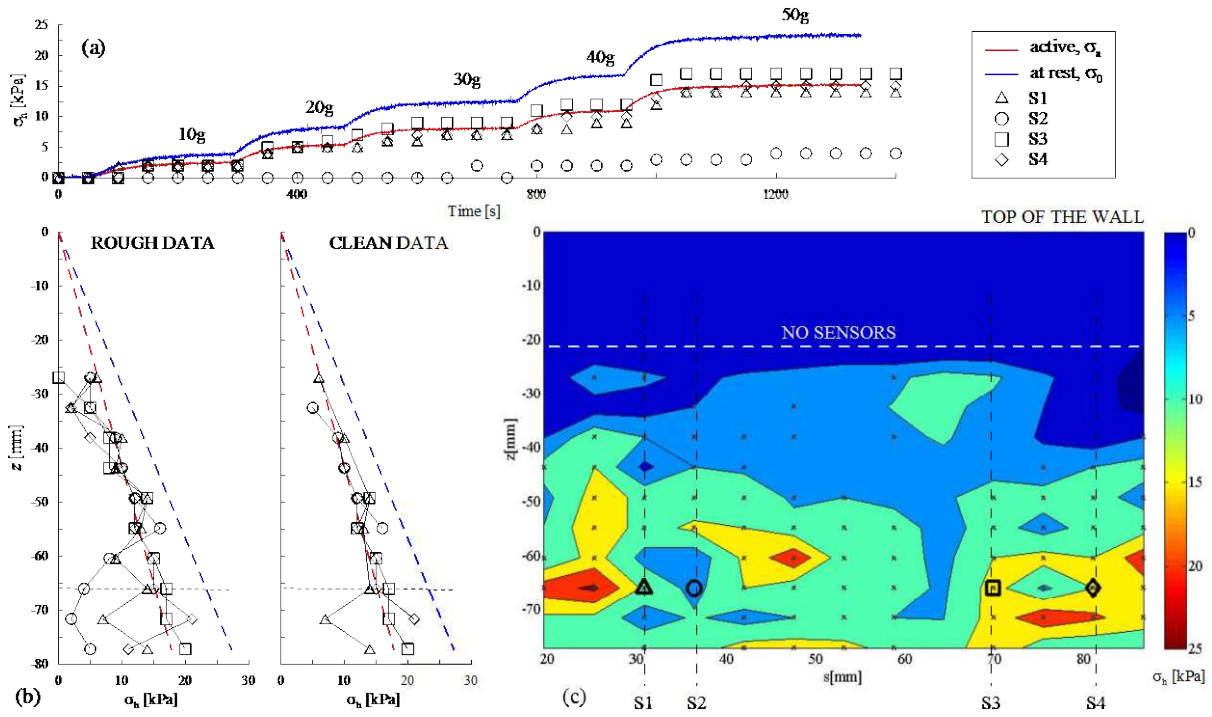

Figure 5. Test VM01, swing up stage.

Dynamic Stage: Kinematic Mechanisms

Figure 6 shows the time history of the horizontal accelerations measured at the base of both the container (A1) and the wall (A2 in test VM01 and A10 in test VM02), the vertical settlements of the backfill (LV3), and the horizontal displacements of the wall measured by transducers LV4 and LV5, located at 10 mm and 49 mm respectively from the top. Only earthquakes EQ3 and EQ4 were considered for test VM01, characterized by approximately the same input accelerations as earthquakes EQ1 and EQ2 in test VM02, both in magnitude and frequency content. As far as the accelerations in the model are concerned, neither amplification phenomena nor phase shift can be appreciated through the sand layer, all the soil experiencing substantially the same acceleration in free field conditions. Looking at wall displacements, three observations are of major concern: (i) in both tests, permanent displacements at the end of the last earthquake are smaller than those recorded during the previous stage; (ii) both rotation and translation of the wall occurred in test VM02; and (iii) horizontal displacements experienced by the wall in test VM02 are significantly larger than those measured in test VM01.

Consistently with the settlement measured by LV3, the first phenomenon is clearly due to a densification of the sand under dynamic loading, resulting in a progressive increase of the strength of the backfill. This is confirmed by Figure 7, which shows a picture of the backfill (a) before and (b) after test VM02. Together with the development of a soil wedge behind the wall, the (initially) loose sand in the backfill clearly densified during the applied earthquakes.

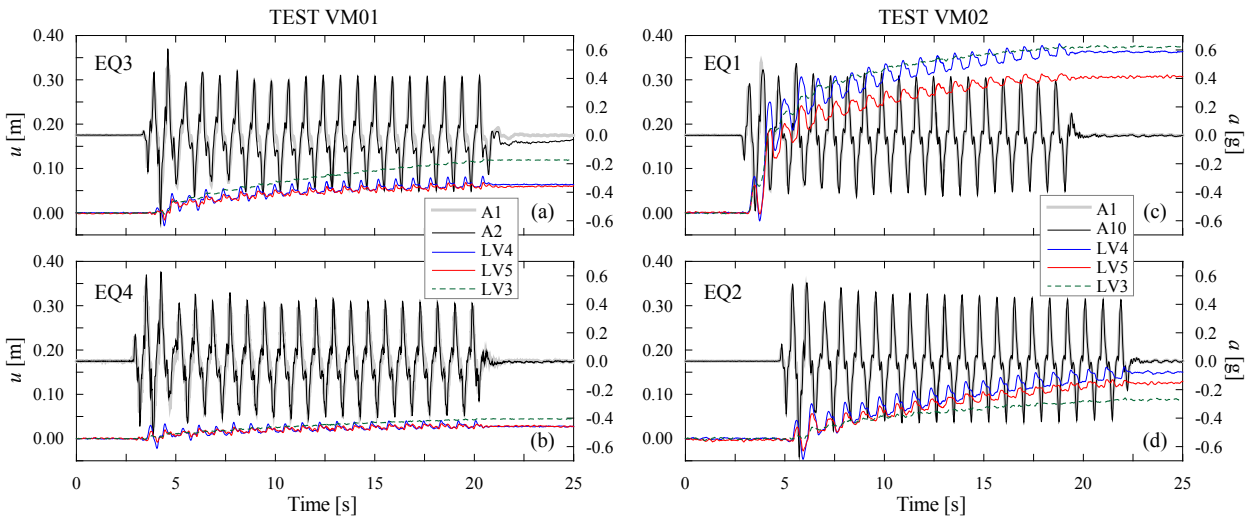

Figure 6. Time history of accelerations and displacements during test VM01, (a) EQ3 and (b) EQ4, and test VM02, (c) EQ1 and (d) EQ2.

The second observation seems to suggest that, contrary to test VM01, where a sliding mechanism was imposed a priori by placing a rigid plate at the base of the wall, a bearing capacity failure mechanism was activated in test VM02. This is further confirmed by inspection of Figure 8, showing the displacement field computed by the PIV analysis in test VM02 during earthquake EQ1, together with the undeformed shape of the wall. The vector displacements close to the toe of the wall are, in fact, those typically associated to a bearing failure of the foundation soil (Knappet *et al*., 2006).

The last observation has significant implications within the light of a Newmark's rigid block analysis. In fact, since the accelerations applied at the base of the wall in the two tests are quite similar, it follows that the yield acceleration in test VM02 should be significantly smaller than in test VM01, *i.e.,* the yield acceleration strongly depends on the kinematic wall mechanism by which displacements occur during the earthquake.

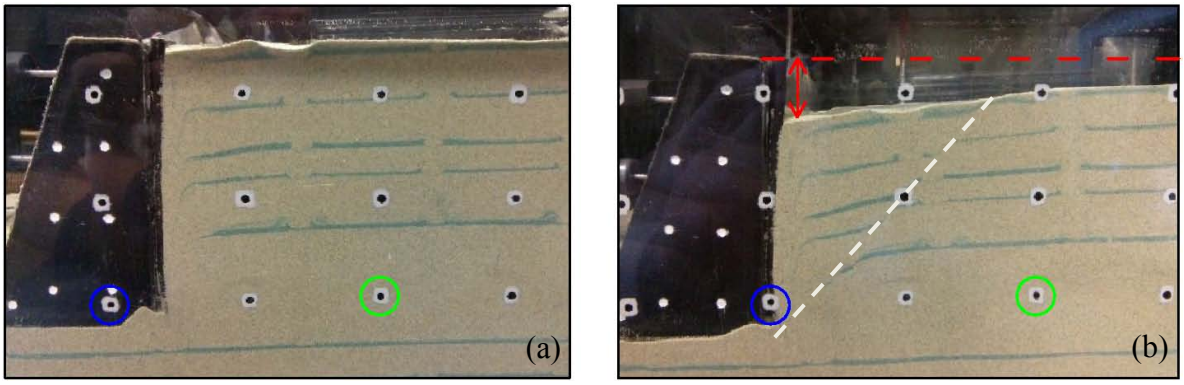

Figure 7. Test VM02: photograph of the model (a) before and (b) after test.

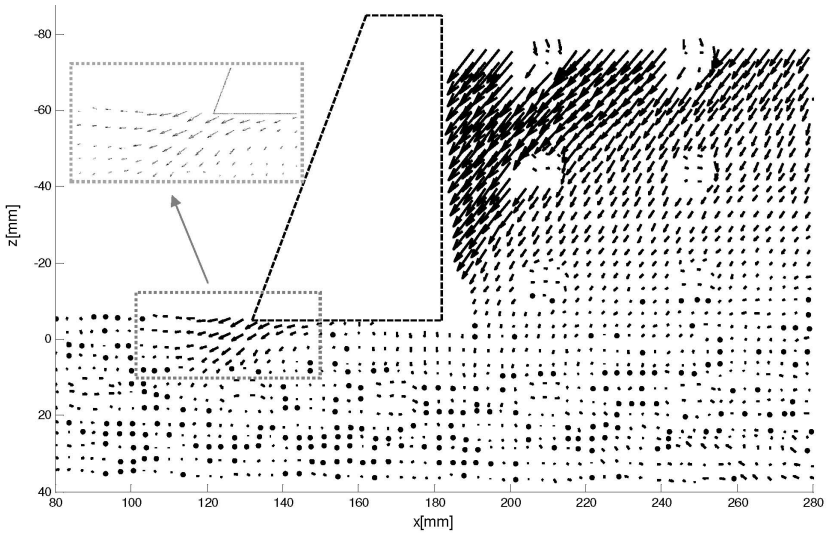

Figure 8. Test VM02, EQ1: displacement field computed by PIV, together with the undeformed shape of the wall.

Conclusions

Two centrifuge dynamic tests on reduced scale models of gravity retaining walls, both supporting a backfill of dry loose sand, were carried out. In test VM01 a rigid plate was placed at the base of the wall in order to force a pure sliding mechanism, while in test VM02 the kinematic mechanism under the dynamic stages was not known a priori. Experimental findings pointed out that a bearing capacity failure mechanism was activated in the latter case. Moreover, based on the applied accelerations and measured displacements, it was concluded that the yield acceleration associated to the attainment of the seismic bearing capacity of the foundation soil is, for the particular case at hand, significantly smaller than that associated to a sliding mechanism.
In the light of a Newmark's rigid-block analysis, these result suggest that care must be taken in computing the yield acceleration of the wall. More in detail, permanent displacements should be computed by taking into account all possible failure mechanisms of the soil-wall system, seeking the most critical for the wall.

Finally, the experimental work was limited to retaining walls in dry sand, and further testing is required to clarify the role of the presence of the pore water.

Acknowledgments

The work presented in this paper was partly funded by the Italian Department of Civil Protection under the ReLUIS research project. The technical support received by Dr. C. Heron and the Technicians of the Schofield Centre is gratefully acknowledged.

References

Conti R., Viggiani G.M.B. (2012). *Evaluation of soil dynamic properties in centrifuge tests*. J. Geotech. Geoenv. Eng., **138**(**7**), 850-859.

Conti R., Viggiani G.M.B., Cavallo S. (2013). *A two-rigid block model for sliding gravity retaining walls*. Soil Dyn. Earth. Eng., **55**, 33-43.

Huang C.C., (2005). *Seismic displacement of soil retaining walls situated on slope*. J. Geotech. Geoenvir. Eng., **131**(9), 1108-1117.

Kloukinas P., Scotto di Santolo A., Penna A., Mylonakis G. (2013). *Experimental investigation of dynamic behaviour of cantilever retaining walls*. COMPDYN 2013, Kos Island, Greece.

Knappet J.A., Haigh S.K., Madabhushi S.P.G. (2006). *Mechanisms of failure for shallow foundations under earthquake loading*. Soil Dyn. Earth. Eng., **26**, 91-102.

Ling, H.I. (2001), *Recent applications of sliding block theory to geotechnical design*. Soil Dyn. Earthquake Eng., **21**(3), 189-197.

Newmark N.M. (1965). *Effects of earthquakes on dams and embankments*. Géotechnique, **15**(2), 139-160.

Richards R., Elms D.G. (1979). *Seismic behaviour of gravity retaining walls*. J. Geotech. Eng. Div., ASCE, **105**(4), 449-464.

Visone, C., Santucci de Magistris, F. (2009). *Mechanical behaviour of the Leighton Buzzard Sand 100/170 under monotonic, cyclic and dynamic loading conditions*. ANIDIS 2009, Bologna, Italy.

White D.J., Take W.A., Bolton M.D. (2003). *Soil deformation measurement using particle image velocimetry (PIV) and photogrammetry*. Géotechnique, **53**(7), 619-631.

Zeng X., Steedman R.S. (2000). *Rotating block method for seismic displacement of gravity walls*. J. Geotech. Geoenv. Eng., **126**(8), 709-717.